# Phase Diagram of Electrostricted $H_2O$ at Surfaces of Electrodes at 273–373 K: Electric Critical Point of Water

Irena Danielewicz-Ferchmin[b] and A. Ryszard Ferchmin*[a]

*The equation of state of an open system containing water in an electric field of strength* E *greater than* $10^8\,\mathrm{V\,m^{-1}}$ *leads to a phase diagram with two-phase and single-phase regions in the* $\Pi$,E,T *coordinates* ($\Pi$ = *electrostriction pressure). The phases differ by their degree of orientation of* $H_2O$ *molecules in the field. The phase transition is discontinuous with respect to* E. *The calculation shows that the discontinuity vanishes at the critical point:* $\Pi_c \approx 0.2$ *GPa,* $E_c \approx 10^9\,\mathrm{V\,m^{-1}}$ *and* $T_c^E$ *below 313 K. The thermal effect of the transition is calculated and compared with an experiment at the Hg/aqueous electrolyte interface found in the literature.*

## 1. Introduction

Understanding the phase behaviour of water in high electric fields still seems to be an open question in physics.[1] Recently, by using the off-specular X-ray scattering technique, it has been possible to reveal phase transitions attributed to a high electric field in a few molecular $H_2O$ layers compressed vertically to the surface of a $RuO_2$ charged electrode.[2] Independently, a theoretical approach to the problem of phase transitions in water under the effect of an electric field has been proposed.[3,4] The approach is based on the equation of state, and follows a thermodynamic law describing the equilibrium state of water placed in a local high electric field of strength $E$ and forming a common system with the remaining water localized outside the field. This equation belongs to the class of so-called rigorous (thermodynamic) equations of state.[5,6]

Some features predicted earlier within the framework of this approach and in agreement with experiment are:

1. In the layers of $H_2O$ at the $Ru_2O$ electrode, a phase transition: normal water (B) → orientationally ordered $H_2O$ phase (A), which was independently predicted by theory,[3,4] has been reported[2] to occur at ambient conditions. Note that some intuition concerning possibly different water phases in high electric fields at ambient conditions seems to have existed for more than a decade: a "solid water layer" at the highly polar $TiO_2$ surface was first reported in 1989.[7]
2. The phase transition B → A (see Table 1) predicted by the theory should occur with a field discontinuity at about $10^9\,\mathrm{V\,m^{-1}}$ (this discontinuity concerns $E(\Pi)$ as a thermodynamic variable depending on the electrostriction pressure $\Pi$—see Section 3). This value coincides with that observed in experiment.[2,8]
3. The predicted changes in entropy $\Delta S$[3] and heat capacity $\Delta C_P$ (ref. [9] and the current paper) at the transitions are of the same order of magnitude as those found by Benderskii et al.[8] using the laser temperature-jump method at a Hg/aqueous electrolyte interface at a field of strength $\approx 10^9\,\mathrm{V\,m^{-1}}$.

Yet another aspect of this phase transition is the relation to the hydrogen bonding (HB) energy. The energy of the electric dipole $\mu = 6\times10^{-30}$ C m of the $H_2O$ molecule in the field $E = 10^9\,\mathrm{V\,m^{-1}}$ characteristic of the transition amounts to $\mu E = 6\times10^{-21}$ J. In other words, this energy is $\approx 4\,\mathrm{kJ\,mole^{-1}}$ of dipoles. The latter quantity should be compared with that of HB energy (20–25 $\mathrm{kJ\,mole^{-1}}$). Thus, the phase transition considered occurs for a value of the local field $E$ in which a dipole has an energy not much below that of the HB energy.

The transition B → A is not accompanied by a density discontinuity. However, with a further rise in $E$, phase A becomes compressed more and more and acquires large density values (twice those of normal water or more).[10]

In an earlier paper,[4] on the basis of the equation of state, we predicted a phase transition in $H_2O$ induced by electrostriction pressure $\Pi_t$ under ambient conditions. The phase transition occurs between partly orientationally ordered water (termed phase B) and a different phase A of $H_2O$, which is orientationally ordered and compressed. In a preliminary short account,[9] we presented theoretical evidence for a phase transition of water in a high field at an electrode at temperature $T$ in the range $273 < T < 303$ K and discussed it in the context of the thermal phenomena observed at a Hg electrode.[8] In that account, the calculations led to the finding of discontinuities in the surface charge density $\sigma$ at a range of temperatures, thus providing evidence for phase transitions from phase B to

---

[a] Prof. A. R. Ferchmin
Institute of Molecular Physics, Polish Academy of Sciences
M. Smoluchowskiego 17, 60-179 Poznań
(Poland)
Fax: (+48) 61-868-4524
E-mail: arfer@ifmpan.poznan.pl

[b] Dr. I. Danielewicz-Ferchmin
Faculty of Physics, A. Mickiewicz University
Umultowska 85, 61-614 Poznań
(Poland)

DOI: 10.1002/cphc.200500106

**Table 1.** The transition electrostriction pressure $\Pi_t$, discontinuities in the electric field strength $\Delta E$, surface charge density $\Delta\sigma$, permittivity $\Delta\varepsilon$ and reduced distance from the centre of an ion $\Delta x$ accompanying the B $\rightarrow$ A transitions at four temperatures $T$.

| $T$ [K] | $\Pi_t$ [GPa] | $\Delta E$ [$10^9$ V m$^{-1}$] | $\Delta\sigma$ [C m$^{-2}$] | $\Delta\sigma$ [$q$ Å$^{-2}$] | $\Delta\varepsilon$ | $\Delta x$ [Å] |
|---|---|---|---|---|---|---|
| 273 | 0.1714 | 0.9254/1.0830 | 0.2662/0.2702 | 0.0166/0.0169 | 32.49/28.18 | 2.187/2.171 |
| 283 | 0.1781 | 0.9742/1.1347 | 0.2666/0.2705 | 0.0167/0.0169 | 30.91/26.92 | 2.185/2.170 |
| 293 | 0.1854 | 1.0253/1.1667 | 0.2675/0.2708 | 0.0167/0.0169 | 29.47/26.22 | 2.182/2.168 |
| 303 | 0.1940 | 1.0819/1.1732 | 0.2692/0.2713 | 0.0168/0.0170 | 28.10/26.12 | 2.175/2.166 |

phase A of $H_2O$ in the field. No discontinuity has been found above the critical temperature $T_c^E = 308 \pm 5$ K.

Herein, we ask the question: what happens to the phase transition B $\rightarrow$ A in $H_2O$ induced by an electrostriction pressure $\Pi_t$[4] in the wider temperature range $273 < T < 373$ K? The ability to answer this question is possible thanks to our earlier calculated permittivity $\varepsilon$ of water as a function of field $E$ and temperature $T$.[11] With respect to the preliminary short account, additional theoretical evidence is presented here; the discontinuities in permittivity $\varepsilon$, local electric field $E$ and distance $x$ from the centre of an ion at the transition are discussed. The calculations are presented in some detail to make the paper self-contained. The critical point $\Pi_c, E_c, T_c^E$ is found in the phase diagram of water in the $(\Pi, E, T)$ variables, where $\Pi$ is the local electrostriction pressure.

Note that on the basis of the thermodynamics only, one cannot decide whether the dense orientationally ordered phase A of water is solid or liquid. If the orientationally ordered and compressed phase A of $H_2O$ was liquid, the present subject would belong to a broader theme of the physics and chemistry of liquids, namely the phase transitions wholly within the liquid state.[1] It is well-known that there exist phase boundaries in the $(P,T)$ plane for quantal ($^4$He, $^3$He and H) and "classical" elemental liquids (C, P, Se, S) characterized by a change in local coordination number across these boundaries.[1] Herein, it is shown that in an open system of water in a high electric field characterized by a finite change in local permittivity $\varepsilon$ across phase boundaries in the $(\Pi, T)$ plane there exists an "electric" critical point $(\Pi_c, T_c^E)$.

Besides those in refs. [2,8], other experiments have been reported that can now be interpreted in the light of the current work as concerning the dense, orientationally ordered phase A of water. The specular X-ray scattering investigation[12] of water at the Ag charged electrode has revealed water layers polarized and compressed to a density as high as twice the normal one, in fields that can now be characterized as higher than those needed for the phase transition under discussion to occur. Its compression has been explained qualitatively by the authors[12] and later quantitatively by others[10] as due to electrostriction.

## 2. Method

In this section, the model applied in the current work is defined and the equation of state of water in a high electric field in the range of temperatures considered is derived. These parameters form the basis for further calculations of the electric-field-induced phase transitions, or strictly speaking those induced by the electrostriction pressure. For the sake of completeness, some details of derivations appearing in our previous work (see ref. [13] for a review) are re-derived in a form suitable for discussing the whole range of temperatures where $H_2O$ is a liquid under atmospheric pressure.

### 2.1. Equilibrium Condition

Water placed in a local high electric field of strength $E > 10^8$ V m$^{-1}$ is encountered in hydration shells of ions, hydration shells around biomolecules and in the double layers at electrodes. It forms a common system with the remaining water localized in a weak field or outside the field. The thermodynamic law describing the state of this system is the equilibrium condition with respect to the mass transport between the regions within and outside the field. The above follows from the condition of equality of the chemical potentials $\zeta$ given by Equation (1):

$$\zeta^{\mathrm{i}} = \zeta^{\mathrm{o}} \tag{1}$$

where the superscripts i and o mark the quantities inside and outside the field, respectively. The chemical potential of the water molecule placed in a high electric field is reduced by $\zeta_W$ due to the work done by the electric field reorienting the electric dipole. To attain an equilibrium, the chemical potential gradient thus created induces the pull of the dipoles into the field and thus produces a compression. We shall deal with a new equilibrium state with water density increased in the high field due to this process. The work $L$ related to water compression in the field—the electrostriction work—enhances the chemical potential of water by $\zeta_L$. After reaching the equilibrium, the latter compensates the negative increment $\zeta_W$ according to Equation (2):

$$-\zeta_W = \zeta_L \tag{2}$$

Herein, it will be shown that the phase transition under ambient conditions described earlier[4] also occurs in the range $273 < T < 303$ K. As before, the question of the transition is considered at the atmospheric pressure ($P^{\circ} = 10^5$ Pa). At $T = 313$ K and higher temperatures, the present approach does not predict any phase transition of the kind: normal water $\rightarrow$ orientationally ordered $H_2O$ (B $\rightarrow$ A).

### 2.2. The Equation of State of $H_2O$ Expressed in the Variables $\Pi$, $E$, $T$

The change in the chemical potential $\zeta_W$ is calculated in a way similar to that described earlier.[4,10,13] In the immediate neighbourhood of the electrode (first layer of water molecules—Helmholtz layer) the field strength $E$ is described by Equation (3):

$$E = \frac{\sigma_0}{\varepsilon_0} = \frac{\sigma}{\varepsilon\varepsilon_0} \tag{3}$$

where $\sigma_0$ is the surface charge density on the electrode, $\varepsilon$ is the permittivity and $\varepsilon_0$ is the permittivity of a vacuum. Similarly, the strength $E$ of the field around the ions (Coulomb field) is given by Equation (3), where [Eq. (4)]:

$$\sigma = \frac{q}{4\pi x^2} \tag{4}$$

and $q$ is the elementary charge, $x$ is a reduced distance from the centre of the ion $x = r \times |Z|^{-1/2}$, $r$ is the distance from the centre of the ion and $Z$ is the number of excess elementary charges of an ion (valence). The work $W$ done by the electric field is given by Equation (5):[10,13]

$$W = \frac{V}{\varepsilon_0} \int_0^y \frac{\sigma}{\varepsilon} \mathrm{d}y \tag{5}$$

where $y = \sigma\left(1 - \frac{1}{\varepsilon}\right)$, $V$ = constant is the volume of the system and $V\mathrm{d}y$ is the increment of the polarization of the whole system. The increment of the grand potential $\Omega$ is given by Equation (6):

$$\mathrm{d}\Omega = -S\mathrm{d}T + EV\mathrm{d}y - N\mathrm{d}\zeta_L \tag{6}$$

where $N$ is the number of molecules in the volume $V$.

Let us introduce the notation [Eq. (7)]:

$$f = \int_0^y \frac{\sigma}{\varepsilon} \mathrm{d}y \tag{7}$$

The work $W$ performed leads to a change $\Delta\Omega$ in the value of the grand potential $\Omega$ of water given by Equation (8):

$$(\Delta\Omega)_{T,V,\zeta_L} = \frac{V}{\varepsilon_0} f \tag{8}$$

For $\zeta_W$, the change in $\zeta$ as a result of the work $W$, one obtains Equation (9):

$$\zeta_W = \left(\frac{\partial\Omega}{\partial N}\right)_{T,V,\zeta_L} \tag{9}$$

The increment is [Eq. (10)]:

$$\zeta_W = \frac{v^\circ N^\circ}{\varepsilon_0} \left(\frac{\partial f}{\partial N}\right)_{\zeta_L} \tag{10}$$

where $v^\circ = V/N^\circ$ and $N^\circ$ is the Avogadro number. It follows from Equation (10) that [Eq. (11)]:

$$\frac{\zeta_W}{v^\circ} = \frac{1}{\varepsilon_0} \left[\left(\frac{\partial f}{\partial y}\right)\left(\frac{\partial y}{\partial \varepsilon}\right)\right]_{\zeta_L} N^\circ \left(\frac{\partial \varepsilon}{\partial N}\right)_y \tag{11}$$

Now, we shall provide some details of the calculation of the right-hand side of Equation (11). The first factor in the form of a derivative is given by Equation (12):

$$\frac{\partial f}{\partial y} = \frac{\sigma}{\varepsilon} = \frac{q}{4\pi\varepsilon x^2} = \frac{qX}{4\pi\varepsilon} \tag{12}$$

where $X = x^{-2}$. The second factor can be written as shown in Equation (13):

$$\frac{\partial y}{\partial \varepsilon} = \frac{q}{4\pi} \left[\left(\frac{\partial X}{\partial \varepsilon}\right)\left(1 - \frac{1}{\varepsilon}\right) + \frac{X}{\varepsilon^2}\right] \tag{13}$$

The third factor $(\partial\varepsilon/\partial N)$ in Equation (11) and $(\partial X/\partial\varepsilon)$ in Equation (13) will be calculated in a way similar to that explained previously.[4,14] From an expression obtained in ref. [11] for permittivity $\varepsilon$ as a function of the field strength $E$ and temperature $T$ (see Equation (23) below), we obtain these derivatives as given by Equations (14):

$$N^\circ \left(\frac{\partial \varepsilon}{\partial N}\right)_y = \frac{\frac{B}{VX(l-1)}\left(l\coth\frac{l\Xi}{l-1} - \coth\frac{\Xi}{l-1}\right)}{\frac{n^2}{\varepsilon^2} - \frac{BA}{VT(l-1)^2(\varepsilon + n^2/2)^2}\left[l^2\left(\sinh\frac{l\Xi}{l-1}\right)^{-2} - \left(\sinh\frac{\Xi}{l-1}\right)^{-2}\right]} \tag{14}$$

and (15):

$$\begin{aligned} \frac{\partial X}{\partial \varepsilon} = X^2 \Bigg\{ & \frac{V(l-1)n^2}{B\varepsilon^2} - \frac{A}{T(l-1)(\varepsilon + n^2/2)^2}\left[l^2\left(\sinh\frac{l\Xi}{l-1}\right)^{-2} \right. \\ & \left. - \left(\sinh\frac{\Xi}{l-1}\right)^{-2}\right]\Bigg\}\Bigg\{\left(\coth\frac{\Xi}{l-1} - l\coth\frac{l\Xi}{l-1}\right) \\ & + \frac{AX}{T(l-1)(\varepsilon + n^2/2)}\left[\left(\sinh\frac{\Xi}{l-1}\right)^{-2} - l^2\left(\sinh\frac{l\Xi}{l-1}\right)^{-2}\right]\Bigg\}^{-1} \end{aligned} \tag{15}$$

where $A$ is given by Equation (16):

$$A = \frac{\mu q(n^2 + 2)}{8\pi k\varepsilon_0}\ \mathrm{m^2\,K} \tag{16}$$

in which $k$ is the Boltzmann constant, $n$ is the refractive index and $B$ is given by Equation (17):

$$B = \frac{4\pi N\mu(n^2+2)}{3q}\ \mathrm{m\,kmole^{-1}} \tag{17}$$

The quantities $A$ and $B$ and the refractive index $n$ are temperature-dependent and found with the help of the data collected in Table 2.

The mean cosine $\langle\cos\theta\rangle$ of the angle $\theta$ between the direction of the external field $E$ and the electric dipole moment $\mu$ of the water molecule for an arbitrary number $l$ of allowed orientations of a dipole is expressed by the Brillouin function[18,19] shown in Equation (18):

$$B_l(\Xi) = \frac{l}{l-1}\coth\frac{l\Xi}{l-1} - \frac{1}{l-1}\coth\frac{\Xi}{l-1} \tag{18}$$

where $\Xi$ is defined as [Eq. (19)]:

$$\Xi = \frac{AX}{T(\varepsilon + n^2/2)} \tag{19}$$

In the framework of our approach[11] the reorientations of dipoles responsible for the high dielectric constant of water can be conceived as due to simultaneous shifts of the proton positions. The structure of the neighbourhood of a hydrogen-bonded molecule, be it traditional fourfold coordinated or, according to a recent study, rather forming chains (twofold strongly bonded coordination),[20] plays a secondary role. In the range $273 < T < 373$ K, the hydrogen-bond energy (20–25 kJ mole$^{-1}$) exceeds the thermal energy $RT$ ($\approx$2–3 kJ mole$^{-1}$) by a factor of about ten. Hence, the very concept of two possible orientations ($l=2$) of water dipoles under ambient conditions seems to be justified. At very high temperatures, in which the thermal energy becomes comparable to the hydrogen-bond energy ($T \approx 3000$ K, $RT \approx 25$ kJ mole$^{-1}$), most of the hydrogen bonds should be broken and the dipoles should be able to rotate freely ($l=\infty$), which induces a behaviour described by the Langevin function $L(\Xi)$. In this context it is natural to look for an interpolation scheme between the two extremes of $\tanh(\Xi)$, corresponding to $l=2$, and $L(\Xi)$, corresponding to $l=\infty$, which represent the upper and lower bounds of $\langle\cos\theta\rangle$, respectively. One of the possible interpolation schemes goes as follows. It is conceivable that in the intermediate temperature range part of the hydrogen bond is disrupted, which implies an intermediate number $l$ of probable directions of the dipole moments lying between two extremes: $2 < l < \infty$. The form of $L(\Xi)$ is obtained from the Brillouin function $B_l(\Xi)$ in the limit ($l \rightarrow \infty$). For small values of the parameter $\Xi$ the function $B_l(\Xi)$ [Eq. (18)] can be expanded into the power series shown in Equation (20):

$$B_l(\Xi) = \frac{l+1}{3(l-1)}\Xi - \frac{l^4-1}{45(l-1)^4}\Xi^3 + \ldots \equiv b(l)\Xi - c(l)\Xi^3 + \ldots \tag{20}$$

The coefficient $b(l)$ and the mean number of orientations $l$ of the dipole moment are interrelated as shown in Equation (21):

$$b(l) = \frac{l+1}{3(l-1)} \tag{21}$$

or inversely as [Eq. (22)]:

$$l = \frac{3b+1}{3b-1} \tag{22}$$

The relation between the permittivity $\varepsilon$ and the electric field strength is, according to the Onsager field model,[21] expressed as Equation (23):

$$\frac{\varepsilon - n^2}{\varepsilon} = \frac{B}{VX}\langle\cos\theta\rangle \tag{23}$$

and Equation (24):

$$\langle\cos\theta\rangle = B_l(\Xi) \tag{24}$$

To find the values of the permittivity $\varepsilon$ in the high electric field $E$ we look for $\langle\cos\theta\rangle = B_l(\Xi)$. To this end, first the numerical value of $b(l)$ [Eqs. (20), (21), (22)] should be found in the linearized version of the Onsager approximation (see ref. [11],

**Table 2.** Values of the mean number $l$ of allowed orientations of $H_2O$ dipoles at temperature $T$ and other quantities entering Equations (23) and (30). $n_D^T$ is the refractive index of water,[15,16] $v$ is the molar volume of water[16] and $\varepsilon$ the dielectric constant of water;[17] $A$ is defined in Equation (16) and $B$ in Equation (17).

| $T$ [K] | $n_D^T$ | $v$ [m$^3$ kmole$^{-1}$] | $\varepsilon$ | $l$ | $A$ [$10^{15}$ m$^2$ K] | $B$ [$10^{-17}$ m kmole$^{-1}$] |
|---|---|---|---|---|---|---|
| 273 | 1.33395 | 0.0180182 | 87.9 | 2.000 | 1.18696 | 3.59355 |
| 283 | 1.33369 | 0.0180207 | 83.96 | 2.010 | 1.18674 | 3.59290 |
| 293 | 1.33299 | 0.0180477 | 80.20 | 2.024 | 1.18615 | 3.59112 |
| 303 | 1.33192 | 0.0180940 | 76.60 | 2.038 | 1.18526 | 3.58841 |
| 313 | 1.33051 | 0.0181566 | 73.17 | 2.052 | 1.18408 | 3.58484 |
| 323 | 1.32894 | 0.0182334 | 69.88 | 2.066 | 1.18277 | 3.58087 |
| 333 | 1.32718 | 0.0183231 | 66.73 | 2.080 | 1.18130 | 3.57642 |
| 343 | 1.32511 | 0.0184249 | 63.73 | 2.095 | 1.17957 | 3.57120 |
| 353 | 1.32287 | 0.0185381 | 60.86 | 2.120 | 1.17771 | 3.56556 |
| 363 | 1.32050 | 0.0186625 | 58.12 | 2.125 | 1.17574 | 3.55961 |
| 373 | 1.31783 | 0.0187980 | 55.51 | 2.140 | 1.17353 | 3.55291 |

Eq. (19) therein) with the help of Equation (25):

$$\frac{3(\varepsilon - n^2)(2\varepsilon + n^2)}{\varepsilon(n^2+2)^2} = b(l)\frac{\mu^2 N^\circ}{\varepsilon_0 v k T} \tag{25}$$

provided that the (field-independent) dielectric constant $\varepsilon$ at a given temperature $T$ is known from experiment. In this way, the values of $b(l)$ are found at a given $T$ (Table 2). Subsequently, by following Equation (22) the values of $l=l(T)$ are found (see Table 2). With the known values of $l(T)$, one finds $B_l(\Xi)$ with the help of Equation (18).

Let us now consider the change in the chemical potential $\zeta_L$ due to the compression work $L$ which, according to Equation (2), will compensate $\zeta_W$. The compression work $L$ is calculated, similarly as in refs. [10,22], by integrating the area under the isotherm $V=V(P)$ where $P$ is pressure on the basis of Equation (26):

$$L = \int_{P^\circ}^{P^i} V(P)\mathrm{d}P \tag{26}$$

The change in the chemical potential $\zeta_L$ due to this work is given by Equation (27):

$$\zeta_L = \frac{\partial}{\partial N}\int_{P^\circ}^{P^i} V(P)\mathrm{d}P = \int_{P^\circ}^{P^i} v(P)\mathrm{d}P \tag{27}$$

where $P^\circ$ denotes the atmospheric pressure. One can rewrite Equation (2) in the form [Eq. (28)]:

$$-\frac{\zeta_W}{v^\circ} = \frac{\zeta_L}{v^\circ} \tag{28}$$

which, by taking into account Equations (11) and (27), is the same as [Eq. (29)]:

$$-\frac{N^\circ}{\varepsilon_0}\left[\left(\frac{\partial f}{\partial y}\right)\left(\frac{\partial y}{\partial \varepsilon}\right)\right]_{\zeta_L}\left(\frac{\partial \varepsilon}{\partial N}\right)_y = \frac{1}{v^\circ}\int_{P^\circ}^{P^i} v(P)\mathrm{d}P \tag{29}$$

The integrals on the right-hand sides of Equations (27) and (29) have been found by substituting the isotherms[23] $v=v(P)$ of water in the liquid state under pressure $P$ in the absence of a field. Of course, the use of the data measured in the absence of the field introduces an approximation. Its validity can only be judged subsequently, as has been done with a positive result in ref. [10]. The upper integral limit [$P^i$, see Eq. (27)] was matched so as to fulfil Equation (29), which is equivalent to putting the pressure value $P^i$ in the field equal to the local electrostriction pressure value $\Pi$ [Eq. (30)]:

$$-\frac{N^\circ}{\varepsilon_0}\left[\left(\frac{\partial f}{\partial y}\right)\left(\frac{\partial y}{\partial \varepsilon}\right)\right]_{\zeta_L}\left(\frac{\partial \varepsilon}{\partial N}\right)_y = \frac{1}{v^\circ}\int_{P^\circ}^{\Pi} v(P)\mathrm{d}P \tag{30}$$

This is the same as saying that the external pressure applied without an electric field would produce water compression comparable to that due to the local electrostriction pressure. Note that a similar position has also been adopted by other authors, e.g. a neutron scattering experiment with isotopic substitution on a 10 M NaOH solution was interpreted to "indicate that ions in aqueous solutions induce a change in water structure equivalent to the application of high pressure".[24]

Equation (30) represents the *equation of state* of $H_2O$ in implicit variables $\Pi$, $E$ and $T$. The dependence on temperature is present through the relation $\varepsilon=\varepsilon(T)$ as expressed in Equation (23) and through introduction into Equation (30) of the isotherm $v=v(P)$ for the same temperature $T$ for which $\varepsilon$ is calculated. The dependence on the electric field strength $E$ is present through $f$ and $y$ [see Eqs. (3)–(7)].

Now, we shall provide some details of the calculation of the right-hand side of the equation-of-state Equation (30). To find its value, the compressibility isotherms every 10 K for $T=273$–373 K were taken from ref. [23]. These data have been plotted (not shown). The plots of Equation (31):

$$d^{-1} = d^{-1}(P) \tag{31}$$

where $d^{-1}$ denotes the relative specific volume $v/v^\circ$, were fitted with fourth-order polynomials [Eq. (32)]:

$$d^{-1} = a + bP + cP^2 + gP^3 + eP^4 \tag{32}$$

where the coefficients of the powers of $P$ are given in Table 3. The integral on the right-hand side of Equation (30) can be written as [Eq. (33)]:

$$\int_{P^\circ}^{\Pi} d^{-1}(P)\mathrm{d}P \tag{33}$$

The polynomials in $P$ (see Equation (32) and Table 3) have been integrated. In this way, the values of $\zeta_L/v^\circ$ [Eq. (28)] as a function of electrostriction pressure $\Pi$ (and, formally, the atmospheric pressure $P^\circ=\text{const.}$) have been obtained. We intended to find the only unknown quantity in Equation (30) for any given (calculated) value of $-\zeta_W/v^\circ=\zeta_L/v^\circ$, namely the electrostriction pressure $\Pi$—the upper limit of the integral on the right-hand side. To this aim, the inverted plots of $\Pi$ versus $\zeta_L/v^\circ$ have been drawn, and yet other polynomials have been fitted to these plots [Eq. (34)]:

$$\Pi = G + H\frac{\zeta_L}{v^\circ} + K\left(\frac{\zeta_L}{v^\circ}\right)^2 \tag{34}$$

where the coefficients are given in (Table 4). Equation (34) enables one to find the value of $\Pi$ for any given value of $-\zeta_W/v^\circ=\zeta_L/v^\circ$ at a given temperature as intended.

**Table 3.** Coefficients occurring in Equation (32) for pressures from $P \geq 10^{-4}$ GPa to those indicated in the last column of this table.

| $T$ [K] | $a$ | $b$ [GPa$^{-1}$] | $c$ [GPa$^{-2}$] | $g$ [GPa$^{-3}$] | $e$ [GPa$^{-4}$] | $P$ [GPa] |
|---|---|---|---|---|---|---|
| 273 | 0.999732 | −0.489379 | 0.64005 | −0.417001 | 0 | $P \leq 0.6$ |
| 283 | 0.999886 | −0.454715 | 0.528748 | −0.31063 | 0 | $P \leq 0.7$ |
| 293 | 1.00102 | −0.4286 | 0.445462 | −0.230999 | 0 | $P \leq 0.8$ |
| 303 | 1.00313 | −0.403163 | 0.350594 | −0.143041 | 0 | $P \leq 1.0$ |
| 313 | 1.00657 | −0.399506 | 0.343901 | −0.139399 | 0 | $P \leq 1.0$ |
| 323 | 1.01069 | −0.399554 | 0.343116 | −0.138654 | 0 | $P \leq 1.0$ |
| 333 | 1.0163 | −0.423661 | 0.454488 | −0.31266 | 0.0853151 | $P \leq 1.5$ |
| 343 | 1.02189 | −0.42902 | 0.459036 | −0.312511 | 0.0844686 | $P \leq 1.5$ |
| 353 | 1.02733 | −0.414078 | 0.368372 | −0.189092 | 0.0373318 | $P \leq 2.0$ |
| 363 | 1.03508 | −0.432433 | 0.398789 | −0.208805 | 0.0415854 | $P \leq 2.0$ |
| 373 | 1.04153 | −0.437349 | 0.401307 | −0.208891 | 0.0413332 | $P \leq 2.0$ |

**Table 4.** Coefficients in Equation (34).

| $T$ [K] | $G$ [$10^9$ Pa] | $H$ [$10^9$ m$^2$] | $K$ [$10^9$ m$^5$ J$^{-1}$] |
|---|---|---|---|
| 273 | −0.000333117 | 1.01479 | 0.164139 |
| 283 | −0.000378811 | 1.01485 | 0.154672 |
| 293 | −0.000471958 | 1.0146 | 0.146068 |
| 303 | −0.000780551 | 1.01625 | 0.135133 |
| 313 | −0.000763445 | 1.01238 | 0.133147 |
| 323 | −0.000879593 | 1.00894 | 0.130785 |
| 333 | −0.00186867 | 1.01581 | 0.113863 |
| 343 | −0.00193153 | 1.01109 | 0.112625 |
| 353 | −0.00377021 | 1.01793 | 0.0994629 |
| 363 | −0.004417 | 1.01392 | 0.09833 |
| 373 | −0.00400114 | 1.00684 | 0.098708 |

## 3. Phase Transition in $H_2O$ Induced by an Electrostriction Pressure $\Pi_t$: The Critical Point

As already shown,[4,13] under *ambient* conditions the values of $E$, $\sigma$, $x$ and $\varepsilon$ show discontinuities at the phase transition from phase B to phase A. We shall discuss what happens to this transition when the temperature is varied while the external pressure remains equal to the atmospheric pressure ($P^o$). Equation (30) is solved with $\Pi$ as the unknown. The $\Pi$,$E$ isotherms obtained on the basis of Equation (30) show discontinuities along the $E$ axis (Figure 1) for 273–303 K, whereas in the range 313–373 K the $\Pi$,$E$ isotherms show no discontinuities.

Let us briefly comment upon this discontinuity. By definition, a first-order transition is characterized by a finite discontinuity in a first derivative of the grand potential $\Omega$ [see Eq. (6)]. In our case, one should expect discontinuities in the following derivatives of $\Omega$ [Eq. (35)]:

$$\frac{1}{V}\left(\frac{\partial\Omega}{\partial y}\right)_{T,V,\xi_L} = E, \quad \left(\frac{\partial\Omega}{\partial T}\right)_{V,\xi_L,y} = -S \tag{35}$$

corresponding to the electric field strength (considered as a thermodynamic variable) and entropy. The plateau of the line $\Pi(E)$ at $\Pi = \Pi_t$ in Figure 1 may, by a simple interchange of the axis $\Pi$ and $E$, be transformed from a horizontal segment into a vertical one, whose length corresponds to the value of the discontinuity of $E$. Of course, this discontinuity as a function of $\Pi$ has nothing to do with a concept of an eventual discontinuity of $E$ *in space*, which could violate the Gauss law.

The $\Pi$ isotherms can also be drawn as a function of the variable $\sigma$ (Figure 2), which is convenient when dealing with charged electrodes or large biomolecules. The additional upper abscissa axis in Figure 2 defines $\sigma$ in units commonly used in biophysics: elementary charge $q$ per Å$^2$ ($q$Å$^{-2}$). The variable $x$ is practical when discussing the phenomena in the neighbourhood of small, nearly spherical ions (Figure 3). Finally, $\Pi$ isotherms are also drawn as a function of permittivity $\varepsilon$ (Figure 4).

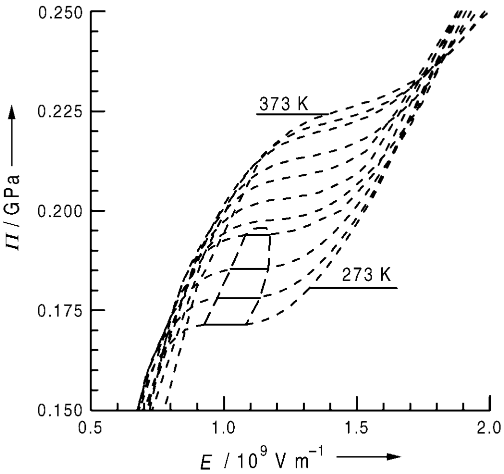

**Figure 1.** Eleven isotherms of electrostriction pressure $\Pi$ [GPa] as a function of electric field $E$ [$10^9$ V m$^{-1}$] plotted every 10 K for temperatures 273–373 K. The apparent straight segments parallel to the $E$ axis correspond to a constant value $\Pi = \Pi_t$ characteristic of the coexistence of phases A and B. The long-dashed line separates the two-phase region from the single-phase region.

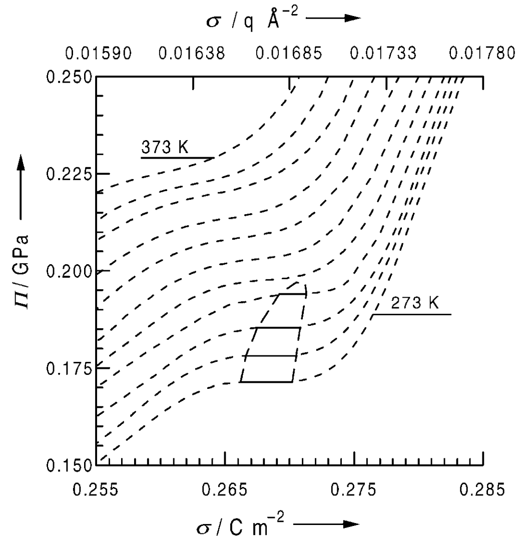

**Figure 2.** Eleven isotherms of electrostriction pressure $\Pi$ [GPa] as a function of surface charge density $\sigma$ [C m$^{-2}$] plotted every 10 K for temperatures 273–373 K. The additional upper abscissa axis defines $\sigma$ in units of elementary charge $q$ per Å$^2$ [$q$ Å$^{-2}$]. The long-dashed line separates a single-phase region from a two-phase region. Within the latter, the values of the electrostriction pressure at straight horizontal segments correspond to a constant value $\Pi = \Pi_t$.

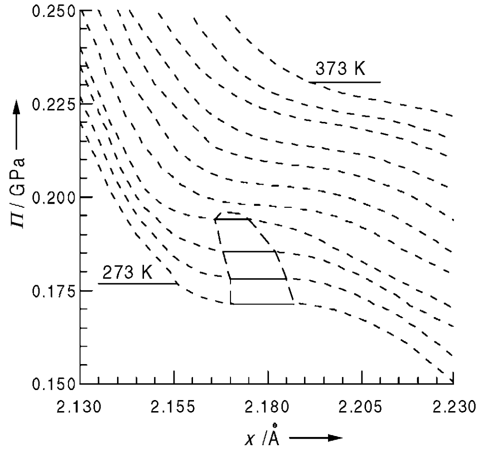

**Figure 3.** Eleven isotherms of electrostriction pressure $\Pi$ [GPa] as a function of the reduced distance $x$ [Å] from the centre of an ion plotted every 10 K for temperatures 273–373 K. The long-dashed line separates a single-phase region from a two-phase region. Within the latter, the values of the electrostriction pressure at straight horizontal segments correspond to a constant value $\Pi = \Pi_t$.

In all the Figures 1–4, for 273–303 K there are apparent straight horizontal segments, characteristic of a domain of coexistence of phases. Along these segments the electrostriction pressure $\Pi$ maintains a constant value $\Pi = \Pi_t$, the transition electrostriction pressure.

In Figure 5 the part of the 273 K isotherm of Figure 1 showing discontinuity is plotted on a very extended scale. On that

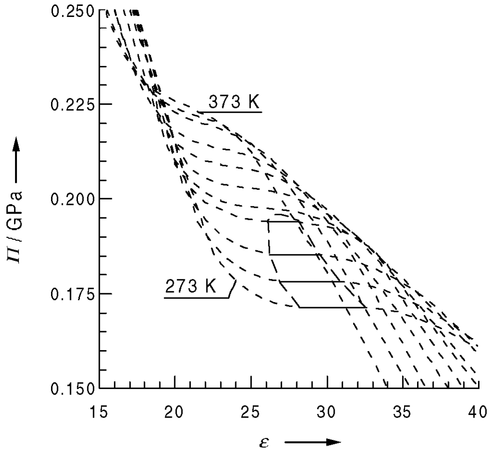

**Figure 4.** Eleven isotherms of electrostriction pressure $\Pi$ [GPa] as a function of permittivity $\varepsilon$ plotted every 10 K for temperatures 273–373 K. The long-dashed line separates a single-phase region from a two-phase region. Within the latter, the values of the electrostriction pressure at straight horizontal segments correspond to a constant value $\Pi = \Pi_t$.

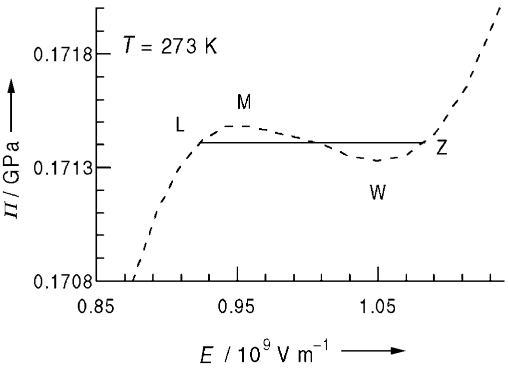

**Figure 5.** Part of the 273 K isotherm of Figure 1 plotted on an extended scale (-----). The portion MW of the isotherm describes a non-physical state, and the portions LM and WZ metastable states. The straight horizontal segment L–Z replacing the wavy LMWZ line describes the thermodynamically stable state with two coexistent phases A and B.

scale one can notice that the segment LZ actually shows a maximum and a minimum. The states corresponding to the portions LM and WZ of the wavy curve are metastable, which is analogous to the situation encountered for van der Waals isotherms. The portion MW of the curve represents unstable states with $(\partial\Pi/\partial E)_T < 0$, which are not physical because they violate the thermodynamic stability conditions. For the system discussed herein, the thermodynamic stability condition is of the form of inequality [Eq. (36)]:

$$\left(\frac{\partial \Pi}{\partial E}\right)_T > 0 \tag{36}$$

since the electrostriction pressure $\Pi$ rises with growing electric field strength $E$. The lengths of the horizontal segments $\Pi = \Pi_t$ of the isotherms are equal to the values of the discontinuities of the electric field $\Delta E$ (Figure 1), surface charge density $\Delta\sigma$ (Figure 2), reduced distance $\Delta x$ from the centre of an ion (Figure 3), or permittivity $\Delta\varepsilon$ (Figure 4, see also Table 1). These horizontal segments shorten with rising temperature: the shortest ones are seen at $T = 303$ K, and at $T \geq 313$ K neither of them is noticeable any more. Above $T = 303$ K an extrapolated line joining the left-hand and the right-hand envelopes of the region of phase coexistence has been drawn. In this way, a line separating the single-phase region from the two-phase region is obtained. The $T$ coordinate of the highest (extrapolated) point of this line corresponds to the *critical temperature* $T_c^E$ lying in the range $303 < T_c^E < 313$ K. Due to the lack of detailed experimental data it was not possible to fix $T_c^E$ more precisely. This "electric" critical temperature $T_c^E$ should be discerned from the usual critical temperature $T_c = 647.069$ K of the liquid–vapour $H_2O$ system in the $P,V,T$ coordinates. The region of coexistence of phases is plotted on an expanded scale in Figure 6. Five electrostriction pressure $\Pi$ isotherms are plotted every 10 K at temperatures ranging from 273 up to 313 K as a function of $E$. The point $T_c^E$ lies on the extrapolated long-dashed line (Figure 6) joining the centres of the straight segments (with $\Pi = \Pi_t$) of the isotherms for four temperatures (see Table 1). On extrapolating this long-dashed line up to the isotherm $(\Pi,E)$ for $T_2 = 313$ K, one finds the point of intersection with the coordinates: $\Pi_2 = 0.198$ GPa and $E_2 = 1.14 \times 10^9$ V m$^{-1}$. They bound the coordinates of the "electric" critical point from above. The coordinates of the centre of the straight segment for $T_1 = 303$ K ($\Pi_1 = 0.194$ GPa, $E_1 = 1.12 \times 10^9$ V m$^{-1}$) bound the critical point from below.

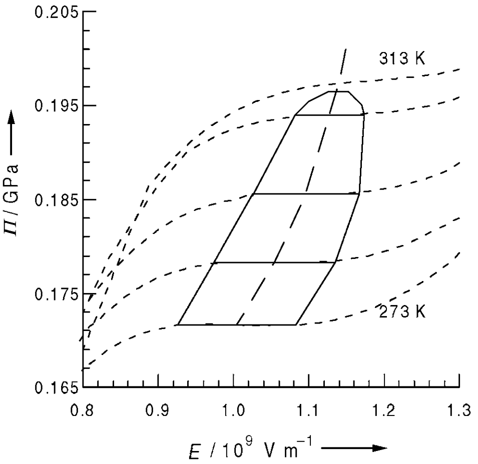

**Figure 6.** Five isotherms of electrostriction pressure $\Pi$ [GPa] as a function of electric field $E$ [$10^9$ V m$^{-1}$]. The isotherms are represented by dashed lines in the single-phase regions and have the form of straight horizontal solid segments in the two-phase region. A long-dashed line going through the centres of these segments is extrapolated up to its intersection with the 313 K isotherm. The two-phase and single-phase regions are separated by a solid line.

The parameters defining the position of the "electric" critical point $\Pi_c, E_c, T_c^E$ are bounded according to the set of inequalities shown in Equation (37):

$$\begin{aligned} &0.194 < \Pi_c < 0.198\,\text{GPa} \\ &1.12 < E_c < 1.14 \times 10^9\,\text{V m}^{-1} \\ &303 < T_c^E < 313\,\text{K} \end{aligned} \tag{37}$$

### 3.1. A Comment on the Numerical Agreement with Previous Work

Note that in ref. [4] the calculated electrostriction pressure at the transition amounted to $\Pi_t = 0.21$ GPa at ambient conditions. This represents a value higher than not only the value $\Pi_t = 0.1854$ GPa (Table 1, column 2) calculated herein at ambient conditions, but also (paradoxically) higher than the highest limit of the transition electrostriction pressure—the upper limit of the critical electrostriction pressure $\Pi_c = 0.198$ GPa, also found herein. The cause of this discrepancy lies in the slightly different model assumptions in ref. [4] and in the current paper. According to the earlier proposed simpler model,[4] there were only two possible directions ($l = 2$, see Table 2, column 5) of the dipole moments.

Herein, the same slightly modified model admits a small temperature-dependent fraction of dipole moments pointing to other directions [see text following Eq. (19)], which results in slightly different values of the permittivity $\varepsilon$ at ambient and other conditions.

## 4. Change in Heat Capacity $\Delta C_P$ at the Phase Transition: Calculated Values and Comparison with Experiment

Thermal phenomena have been observed at the mercury/aqueous electrolyte interface by the laser temperature-jump method.[8,25] They were reported as accompanying a phase transition in the field of strength of $10^9$ V m$^{-1}$. Values of $\Delta C_P$ equivalent to several J mole$^{-1}$ K$^{-1}$ have been found. We shall now calculate $\Delta C_P$ within our approach and compare it with the above-mentioned experiment. To this aim, the coexistence line of the phases A and B will be plotted, its tangent found and a formula analogous to the Clausius–Clapeyron law applied. To obtain the coexistence line, the region $(\Pi,\sigma,T)$ of coexistence of phases A and B (Figure 7) was projected onto the $(\Pi,T)$ plane. The coexistence line is plotted as a full line in Figure 8.

The ordinates of the four points (full symbols) marked on this line correspond to the values of $\Pi_t$ (see Table 1) at temperatures 273, 283, 293 and 303 K. The "electric" critical point $(\Pi_c, T_c^E)$ is situated at the end of the coexistence line, within the rectangle C with the corners at the points $(\Pi_1,T_1)$, $(\Pi_1,T_2)$, $(\Pi_2,T_2)$ and $(\Pi_2,T_1)$ (see Figure 8). The change in heat capacity $\Delta C_P$ at the transition between the phases B and A was calculated by following the Clausius–Clapeyron-like Equation (38):

$$\frac{d\Pi}{dT} = \frac{\Delta S}{\Delta v} \tag{38}$$

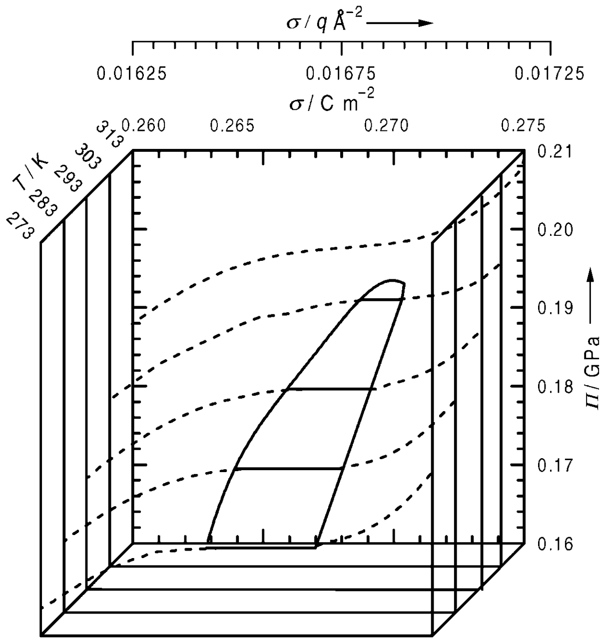

**Figure 7.** The region of coexistence of phases in three dimensions: $\Pi$, $\sigma$ and $T$. The additional upper abscissa axis defines $\sigma$ in units $q\,\text{Å}^{-2}$. The solid line separates a single-phase region from a region in which the phases A and B of $H_2O$ coexist. There are apparent isotherms containing straight horizontal segments at $\Pi = \Pi_t$. The highest temperature at which such a straight segment can be noticed is $T = 303$ K; for $T = 313$ K it is not apparent.

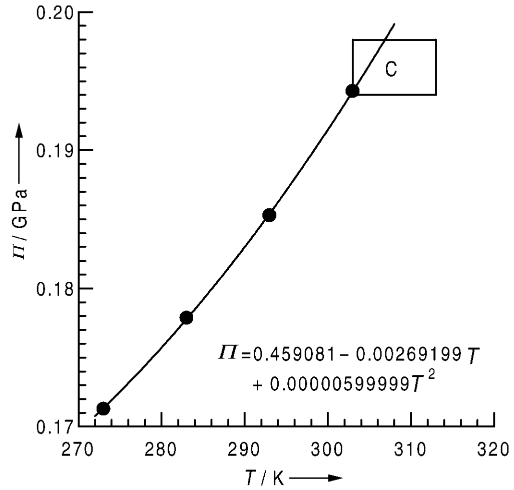

**Figure 8.** Coexistence line of phases A and B. The critical point $\Pi_c, T_c^E$ is situated at the end of the coexistence line, within the rectangle C drawn between 303 and 313 K, as well as between electrostriction pressures 0.194 and 0.198 GPa. The second-order equation fitted to the coexistence line is written in the figure.

where the electrostriction pressure $\Pi$ replaces the common mechanical pressure $P$. For the phase transition calculated herein, $\Delta v = 0$ (see ref. [13]). Under adiabatic conditions, by making use of the well-known thermodynamic identities between partial differential coefficients,[26] Equation (38) can be expressed as Equation (39) (see ref. [27], Chap. 4, §4):

$$\Delta C_P = \frac{d\Pi}{dT} T v(\Delta\alpha) \tag{39}$$

where $\Delta\alpha$ is the change in the coefficient of thermal expansion at the transition. We will calculate $\Delta C_P$ for two temperatures: 293 and 303 K. From the equation of the second-order polynomial (shown in Figure 8) fitted to the four points in Figure 8, the values of $d\Pi/dT$ were calculated from Equations (40):

$$\left(\frac{d\Pi}{dT}\right)_{293} = 8.2 \times 10^{-4}\ \text{GPa}\,\text{K}^{-1} \tag{40}$$

and (41):

$$\left(\frac{d\Pi}{dT}\right)_{303} = 9.4 \times 10^{-4}\ \text{GPa}\,\text{K}^{-1} \tag{41}$$

Now, it will be shown how to estimate the values of $v(\Delta\alpha)$ in Equation (39). The relations $v = v(T)$ (Figure 9) were plotted on the basis of the data of ref. [23] for $P = 0.18$ and 0.20 GPa. These are the closest values of pressure $P$ with respect to the values of the electrostriction pressures $\Pi_t = 0.1854$ and 0.1940 GPa (see Table 1) for which experimental data of $v = v(T)$ are available. From the slope differences of the pairs of lines (see Figure 9), the values of $v(\Delta\alpha)$ in Equations (42) and (43) have been found:

$$[v(\Delta\alpha)]_{293} = 0.23 \times 10^{-6}\ \text{m}^3\,\text{kg}^{-1}\,\text{K}^{-1} \tag{42}$$

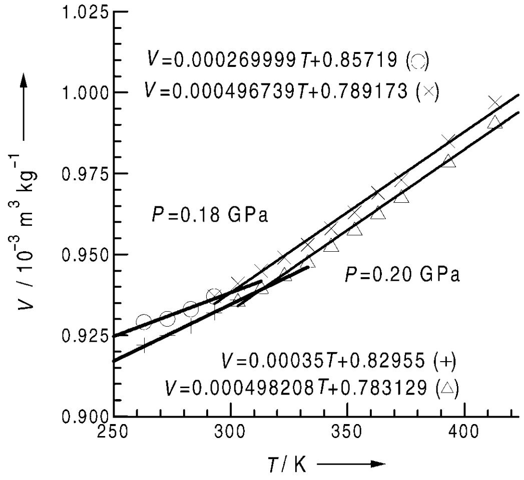

**Figure 9.** The specific volume $V$ [$10^{-3}\ \text{m}^3\text{kg}^{-1}$] as a function of temperature $T$ plotted on the basis of the data of ref. [23] for pressure $P = 0.18$ GPa (upper line) and 0.20 GPa (lower line). For $P = 0.18$ GPa, in the range $263 < T < 293$ K the relation $V = V(T)$ has been approximated by a straight line fitted to the empty circles, and in the range $293 < T < 413$ K by another one fitted to the crosses (×). For $P = 0.20$ GPa, in the range $263 < T < 293$ K the relation $V = V(T)$ has been approximated by another straight line fitted to the (+) signs, and in the range $293 < T < 413$ K by yet another line fitted to the empty triangles. The equations $V = V(T)$ shown in the figure are the equations of these lines.

and:

$$[v(\Delta\alpha)]_{303} = 0.15\times 10^{-6}\,\mathrm{m^3\,kg^{-1}\,K^{-1}} \quad (43)$$

We found from Equation (39) [Eqs. (44) and (45)]:

$$(\Delta C_P)_{293} = 1.0\,\mathrm{J\,mole^{-1}\,K^{-1}} \quad (44)$$

and

$$(\Delta C_P)_{303} = 0.8\,\mathrm{J\,mole^{-1}\,K^{-1}} \quad (45)$$

Note that with temperatures approaching $T_c^E$ from below, the above changes in heat capacity $\Delta C_P$ at constant pressures [see Eqs. (44) and (45)] at the transitions diminish and should vanish above $T_c^E$ since there are no more transitions at such temperatures. Indeed, Benderskii et al.[8] observed vanishing of $\Delta C_P$ at a temperature of about 323 K, which is only slightly higher than the upper limit $T_c^E = 308+5$ K of the critical temperature found herein with uncertainty taken into account. The above values of $\Delta C_P$ are comparable (on the order of magnitude) to the changes in heat capacity at constant pressure that were found by Benderskii et al.[8]

Let us recall that our approach concerns water. This means that the present results, including the value of the critical temperature $T_c^E$, should essentially remain unaffected by the choice of the aqueous electrolyte and electrode material. Testing of this prediction, e.g. by extending the experiments of Benderskii et al.[8] on Hg/aqueous NaF electrolyte interfaces to other systems, would be welcome. Care should be taken, however, to assure the appropriate values of the electric field within the double layer.

## 5. Discussion and Conclusions

A model approach to water in a high electric field has recently led to a prediction of a phase transition in $H_2O$ in a local field strength of $\approx 10^9\,\mathrm{V\,m^{-1}}$ at ambient conditions [3,4] that was found to be in agreement with experiment.[2,8] Herein, we have studied this phase transition with the previous approach extended to cover the whole temperature range of $H_2O$ existence as a liquid. We have found that the phase transition related to the electric quantities ($E$, $\sigma$, $x$, $\varepsilon$) previously found at ambient temperature actually occurs in the range of $273 \leq T \leq 303$ K. The existence of an entropy discontinuity at the transition (latent heat at ambient temperature) was found in our previous work. The existence of the transition has been corroborated herein in another way, namely from a Clapeyron–Clausius-like equation giving the increment $\Delta C_P$. We have presented *theoretical evidence* of an "electric" critical temperature $T_c^E = 308 \pm 5$ K at which the borderline of the two-phase region reaches its highest point. The *experimental evidence* of the upper bound of the phase transition at $T_c^E$ can be seen as a vanishing at about 323 K of the transition thermal effect observed in ref. [8].

Earlier, we published results concerning permittivity in the field above $10^8\,\mathrm{V\,m^{-1}}$ in the whole temperature range of $H_2O$ existence as a liquid, and found in an abrupt fall of $\varepsilon$ at $E \approx 10^9\,\mathrm{V\,m^{-1}}$ leading, with further rising field, to the temperature-independent state of dielectric saturation.[11] If the electrostriction pressure $\Pi$ (see Figure 4) is plotted as a function of permittivity $\varepsilon$, we find a jump (discontinuity) in $\varepsilon$ for a transition value $\Pi_t$ of the electrostriction pressure corresponding to the field $E \approx 10^9\,\mathrm{V\,m^{-1}}$ (see Table 1). Our present analysis shows that this feature persists up to the critical temperature $T_c^E$ and vanishes above it (see Figure 4).

The very existence of the "electric" critical point ($\Pi_c, E_c, T_c^E$) leads immediately to the asking of a basic question concerning the nature of the phases A and B between which the transition occurs. We have already noted in the Introduction that within our purely thermodynamic approach on basic grounds one can say nothing on the structure of the phases taking part in the transition. Also, experimental evidence has been cited which speaks in favour of the idea that one of the phases (A) might be solid. However, this leads to yet another question of how to conceive the nature of $H_2O$ above $T_c^E$, where one cannot discern between the two phases any more. The answer requires further study.

**Keywords:** electrochemistry · liquids · phase diagrams · thermodynamics · water chemistry

[1] G. G. N. Angilella, F. E. Leys, N. H. March, R. Pucci, *Phys. Chem. Liq.* **2003**, *41*, 211 – 226.

[2] Y. S. Chu, T. E. Lister, W. G. Cullen, H. You, Z. Nagy, *Phys. Rev. Lett.* **2001**, *86*, 3364 – 3367.

[3] I. Danielewicz-Ferchmin, A. R. Ferchmin, *Chem. Phys. Lett.* **2002**, *351*, 397 – 402; errata ibid. **2002**, *358*, 357.

[4] I. Danielewicz-Ferchmin, A. R. Ferchmin, *Phys. Chem. Chem. Phys.* **2003**, *5*, 165 – 171.

[5] H. S. Frank, *J. Chem. Phys.* **1955**, *23*, 2023 – 2032.

[6] G. W. Toop, *Metall. Mater. Trans. B* **1995**, *26*, 577 – 580.

[7] J. J. Kasinski, L. A. Gomez-Jahn, K. J. Faran, S. M. Gracewski, R. J. Dwayne Miller, *J. Chem. Phys.* **1989**, *90*, 1253 – 1269.

[8] V. A. Benderski, A. M. Brodsky, G. I. Velichko, L. I. Daikhin, N. S. Lidorenko, G. F. Muchnik, *Dokl. Akad. Nauk SSSR* **1986**, *286*, 648 – 652.

[9] I. Danielewicz-Ferchmin, A. R. Ferchmin, *Chem. Phys. Lett.* **2004**, *398*, 186 – 189.

[10] I. Danielewicz-Ferchmin, A. R. Ferchmin, *J. Phys. Chem.* **1996**, *100*, 17 281 – 17 286.

[11] I. Danielewicz-Ferchmin, A. R. Ferchmin, *Phys. Chem. Chem. Phys.* **2004**, *6*, 1332 – 1339.

[12] M. F. Toney, J. N. Howard, J. Richer, G. L. Borges, J. G. Gordon, O. R. Melroy, D. G. Wiesler, D. Yee, L. B. Sorensen, *Nature* **1994**, *368*, 444 – 446.

[13] I. Danielewicz-Ferchmin, A. R. Ferchmin, *Phys. Chem. Liq.* **2004**, *42*, 1 – 36.

[14] I. Danielewicz-Ferchmin, A. R. Ferchmin, *J. Chem. Phys.* **1998**, *109*, 2394 – 2402.

[15] *Spravochnik Khimika, vol. 1* (Ed.: B. P. Nikol'skiy), 3rd corrected ed., Izd. Khimiya, Leningrad, **1971**, p. 1029 (Russ.).

[16] *Handbook of Chemistry and Physics* (Ed.: R. C. Weast), 67th ed., CRC Press, Boca Raton, FL, **1986–1987**.

[17] D. P. Fernández, Y. Mulev, A. R. H. Goodwin, J. M. H. Levelt Sengers, *J. Phys. Chem. Ref. Data* **1995**, *24*, 33 – 69.

[18] C. Kittel, *Introduction to Solid State Physics*, Wiley, New York, **1966**, Chap. 14.

[19] J. S. Smart, *Effective Field Theories of Magnetism*, W. B. Saunders, Philadelphia, **1966**, Chap. 1.

[20] Ph. Wernet, D. Nordlund, U. Bergmann, M. Cavalleri, M. Odelius, H. Ogasawara, L. Å. Näslund, T. K. Hirsch, L. Ojamäe, P. Glatzel, L. G. M. Pettersson, A. Nilsson, *Science* **2004**, *304*, 995 – 999.

[21] C. J. F. Böttcher, O. C. Van Belle, P. Bordevijk, A. Rip, *Theory of Electric Polarization, vol. 1*, 2nd ed., Elsevier, Amsterdam, **1973**.

[22] I. Danielewicz-Ferchmin, A. R. Ferchmin, *Physica B* **1998**, *245*, 34–44.

[23] *Handbook of Physical Constants* (Ed.: S. P. Clark), revised edn., The Geological Society of America, New York, **1966**.

[24] F. Bruni, M. A. Ricci, A. K. Soper, *J. Chem. Phys.* **2001**, *114*, 8056–8063.

[25] A. M. Brodsky, L. I. Daikhin, *Elektrokhimiya* **1989**, *25*, 435–451.

[26] E. A. Guggenheim, *Thermodynamics*, North-Holland, Amsterdam, **1957**.

[27] A. R. Ubbelohde, *Melting and Crystal Structure*, Clarendon Press, Oxford, **1965**. (Russ. translation, Mir, Moscow, **1969**).

Received: February 21, 2005
Revised: May 14, 2005